HHS Public Access

Author manuscript

Radiother Oncol. Author manuscript; available in PMC 2022 April 25.

Published in final edited form as:

Radiother Oncol. 2021 October ; 163: 199–208. doi:10.1016/j.radonc.2021.08.012.

Radiation therapy related cardiac disease risk in childhood cancer survivors: Updated dosimetry analysis from the Childhood Cancer Survivor Study

Suman Shrestha[a,b], **James E. Bates**[c], **Qi Liu**[d], **Susan A. Smith**[a], **Kevin C. Oeffinger**[e], **Eric J. Chow**[f], **Aashish C. Gupta**[a,b], **Constance A. Owens**[a,b], **Louis S. Constine**[g], **Bradford S. Hoppe**[h], **Wendy M. Leisenring**[f], **Ying Qiao**[a], **Rita E. Weathers**[a], **Laurence E. Court**[a,b], **Chelsea C. Pinnix**[i], **Stephen F. Kry**[a,b], **Daniel A. Mulrooney**[j,k], **Gregory T. Armstrong**[k], **Yutaka Yasui**[k,1], **Rebecca M. Howell**[a,b,*,1]

[a]Department of Radiation Physics, The University of Texas MD Anderson Cancer Center, United States

[b]The University of Texas MD Anderson Cancer Center UTHealth Graduate School of Biomedical Sciences, United States

[c]Department of Radiation Oncology, Winship Cancer Institute, Emory University, United States

[d]University of Alberta, Canada

[e]Department of Medicine, Duke University School of Medicine

[f]Clinical Research and Public Health Sciences Divisions, Fred Hutchinson Cancer Research Center

[g]Department of Radiation Oncology and Pediatrics, University of Rochester Medical Center

[h]Department of Radiation Oncology, Mayo Clinic Florida

[i]Department of Radiation Oncology, The University of Texas MD Anderson Cancer Center

[j]Oncology Department, St. Jude Children's Research Hospital, United States

[k]Department of Epidemiology and Cancer Control, St. Jude Children's Research Hospital, United States

Abstract

Background and purpose: We previously evaluated late cardiac disease in long-term survivors in the Childhood Cancer Survivor Study (CCSS) based on heart radiation therapy (RT) doses estimated from an age-scaled phantom with a simple atlas-based heart model (H_{Atlas}). We enhanced our phantom with a high-resolution CT-based anatomically realistic and validated age-

*Corresponding author at: Department of Radiation Physics, The University of Texas, MD Anderson Cancer Center, United States. rhowell@mdanderson.org (R.M. Howell).

[1]Co-senior author.

Appendix A. Supplementary data

Supplementary data to this article can be found online at https://doi.org/10.1016/j.radonc.2021.08.012.

scalable cardiac model (H_{Hybrid}). We aimed to evaluate how this update would impact our prior estimates of RT-related late cardiac disease risk in the CCSS cohort.

Methods: We evaluated 24,214 survivors from the CCSS diagnosed from 1970 to 1999. RT fields were reconstructed on an age-scaled phantom with H_{Hybrid} and mean heart dose (D_m), percent volume receiving ≥ 20 Gy (V_{20}) and ≥ 5 Gy with $V_{20} = 0$ ($V_{5,(V20=0\%)}$)were calculated. We reevaluated cumulative incidences and adjusted relative rates of grade 3–5 Common Terminology Criteria for Adverse Events outcomes for any cardiac disease, coronary artery disease (CAD), and heart failure (HF) in association with D_m, V_{20}, and $V_{5,(V20=0\%)}$ (as categorical variables).

Dose-response relationships were evaluated using piecewise-exponential models, adjusting for attained age, sex, cancer diagnosis age, race/ethnicity, time-dependent smoking history, diagnosis year, and chemotherapy exposure and doses. For relative rates, D_m was also considered as a continuous variable.

Results: Consistent with previous findings with H_{Atlas}, reevaluation using H_{Hybrid} dosimetry found that, D_m ≥ 10 Gy, V_{20} ≥ 0.1%, and $V_{5,(V20=0\%)}$ ≥ 50% were all associated with increased cumulative incidences and relative rates for any cardiac disease, CAD, and HF. While updated risk estimates were consistent with previous estimates overall without statistically significant changes, there were some important and significant ($P < 0.05$) increases in risk with updated dosimetry for D_m in the category of 20 to 29.9 Gy and V_{20} in the category of 30% to 79.9%. When changes in the linear dose–response relationship for D_m were assessed, the slopes of the dose response were steeper ($P < 0.001$) with updated dosimetry. Changes were primarily observed among individuals with chest-directed RT with prescribed doses ≥ 20 Gy.

Conclusion: These findings present a methodological advancement in heart RT dosimetry with improved estimates of RT-related late cardiac disease risk. While results are broadly consistent with our prior study, we report that, with updated cardiac dosimetry, risks of cardiac disease are significantly higher in two dose and volume categories and slopes of the Dm-specific RT-response relationships are steeper. These data support the use of contemporary RT to achieve lower heart doses for pediatric patients, particularly those requiring chest-directed RT.

Keywords

Late effects; Radiation therapy; Cardiac toxicity; Childhood cancer; Outcome; Modeling; Cardiac Disease

---

Childhood cancer survivors are at risk for developing multiple treatment-related cardiac diseases, including heart failure (HF), coronary artery disease (CAD), valvular disease, arrhythmia, and pericardial disease [1,2]. Previous cohort studies of childhood cancer survivors have established dose–response relationships between cardiac disease and radiation therapy (RT) [2–7]. The largest cohort for which such relationships have been reported is the Childhood Cancer Survivor Study (CCSS), which recently demonstrated that the risk for late cardiac disease increases with increasing mean heart dose (D_m), increasing heart volume receiving ≥ 20 Gy (V_{20}), and when more than half of the heart volume receives ≥ 5 Gy, but < 20 Gy ($V_{5,(V20=0\%)}$)[4].

In that prior study [4], we estimated heart dose and dose-volume metrics for participants in the CCSS by reconstructing each individual's RT on a computational phantom scaled to their age at RT. Dose reconstruction was necessary because the majority of these survivors were treated in the pre-computed tomography (CT) era of RT. The cardiac model (H_{Atlas}) in our computational phantom at the time of that study was based on manual translation of the size, shape, and placement of the heart from a cross-sectional anatomy atlas to our phantom [8,9]. Recently, we developed an enhanced high-resolution CT-based anatomically realistic age-scalable cardiac model (H_{Hybrid}) [10]. We previously demonstrated that our enhanced cardiac model is valid from infant to adolescent (and superior to H_{Atlas}) when compared to the gold standard CT based voxelized pediatric phantoms [10]. The purpose of this study was to update our previously reported RT-related late cardiac disease risk for the CCSS using doses calculated with the enhanced heart model, H_{Hybrid} (as opposed to H_{Atlas}).

Methods

Study design

We previously reported RT-related late cardiac disease risk in the CCSS using H_{Atlas} [4]. Here, we recomputed the heart doses for the CCSS cohort using the same age-scaled computational phantom, but with an updated CT-based anatomically realistic and validated heart model (H_{Hybrid}) [10]. For comparison H_{Atlas} and H_{Hybrid} are illustrated in Supplementary Fig. 1. Our general methodology for RT record abstraction, dose reconstruction [9,11,12], and heart dose calculations [10], which include dose from direct and stray radiation, has been described elsewhere. To study the impact of updated cardiac model on RT-dosimetry, differences in D_m, V_5 and V_{20} were calculated for each individual in the CCSS cohort who received RT. The data was stratified by primary cancer diagnosis. To study and illustrate the impact of updated dosimetry, scatterplots and histogram of differences were created. Additionally, 99^{th} and 90^{th} percentile decrease was calculated to identify subgroups for whom there were largest change/impact in dosimetry.

Dose-response analyses were repeated with the updated dose and dose-volume metrics, which included D_m, V_{20}, and $V_{5,(V20=0\%)}$. Consistent with our previous analysis, we limited analysis of V_5 data to those receiving less than 20 Gy to any portion of their heart to identify survivors receiving only low to moderate RT doses. Only RT data were updated in this analysis, all other data and parameters remained the same as in our previous study [4] and are briefly summarized below.

Participants

The CCSS is a multi-institutional retrospective cohort study of pediatric cancer survivors, diagnosed (before the age of 21 years) with leukemia, central nervous system tumor, Hodgkin lymphoma, non-Hodgkin lymphoma, kidney tumor, neuroblastoma, soft tissue sarcoma, and bone cancer between January 1, 1970, and December 31, 1999, from 31 participating institutions (in the United States and Canada) who survived at least 5 years from primary cancer diagnosis. The CCSS methodology and participation characteristics have been previously described [13–15]. The original population evaluated in Bates et al. [4] included 24,355 participants from 27 of the 31 institutions. In that study, we excluded

141 participants who developed cardiac disease within 5 years of primary cancer diagnosis, resulting in 24,214 participants; of those 11,960 received RT and had sufficient data for H_{Atlas} heart dose reconstruction [4]. In this analysis, we used the same population except excluded an additional 41 of the 11,960 participants (0.34%) treated with RT, because during quality assurance of the dosimetry data, we determined that there were treatment field uncertainties that precluded accurate dose calculations for the higher resolution (H_{Hybrid}) model. In total, 24,173 participants were included in this analysis, 11,919 of whom were treated with RT.

Late cardiac disease outcomes

We used the same cardiac outcomes as in our previous study [4], which are briefly summarized here. Cardiac outcomes were reported as part of a series of multi-item, organ system based CCSS questionnaires (available at http://ccss.stjude.org). The reported outcomes were classified according to the National Cancer Institute Common Terminology Criteria for Adverse Events (version 4.03), as mild (grade 1), moderate (grade 2), severe or disabling (grade 3), life-threatening (grade 4), or fatal (grade 5). Only conditions graded 3–5 were included in both our current and previous analyses. In our prior study there were 658 participants who reported one or more cardiac condition, including 371 with HF, 304 with CAD, 96 with arrhythmia, 70 with valvular disease, and 28 with pericardial disease [4]; participants who developed any one of those conditions were identified as having any cardiac disease. After excluding the 41 participants for whom we could not perform H_{Hybrid} dosimetry, our present analysis included 652 participants with one or more cardiac conditions, 368 with HF, 301 with CAD, 94 with arrhythmia, 69 with valvular disease, and 28 with pericardial disease. In both our current and previous analyses, we analyzed risks of developing any cardiac disease, CAD, and HF.

Statistical analysis

Incidence of any cardiac disease, CAD, and HF was determined using the identical time-to-event analysis methods as our previous analysis, starting the time at-risk at five years from primary cancer diagnosis, treating death, second malignant neoplasm, and recurrence of the primary cancer as competing risk events. We then created cumulative incidence curves stratified by each dose metric, D_m, V_{20}, and $V_{5,(V20=0\%)}$, calculated using H_{Atlas} and H_{Hybrid} [16]. We used piecewise exponential models to assess the adjusted incidence rate of each outcome in association with each of the three dose-volume metrics calculated by each heart model, adjusting for attained age, sex, age at cancer diagnosis, race/ethnicity, time-dependent smoking history, diagnosis year, and chemotherapy exposure and doses. To assess statistical significance of the differences between results using H_{Atlas} versus H_{Hybrid}, we compared the cumulative incidences at 30 years after primary cancer diagnosis and the adjusted relative rates by resampling with replacement (bootstrapping) individual survivors in the current-analysis dataset using the bootstrap percentile method [17]. Specifically, in each of the 1000 iterations of the bootstrap, we used both the H_{Atlas} and H_{Hybrid} dosimetry datasets on the same bootstrapped sample of survivors and obtained the respective cumulative incidences and adjusted relative rates. The differences were then assessed for their sampling variations across the 1000 iterations to infer their statistical significance. We

provide all data on D_m, V_5, V_{20} and their associations with all three outcomes (any cardiac disease, CAD, and HF) comprehensively, instead of reporting them separately, which is a report on multiple hypotheses of interest and should not be viewed as multiple testing of a single hypothesis.

To examine the effect of updated dosimetry on the slopes of the D_m-specific RT-response relationships, we fitted the same piecewise exponential model above with D_m as a continuous variable. We plotted the adjusted relative rate estimates with their 95% confidence intervals (CIs) for the four D_m categories for any cardiac disease, CAD, and HF, estimated with H_{Hybrid} and H_{Atlas} dosimetry, where the median dose of each D_m category (according to H_{Hybrid} and H_{Atlas}) was used as the representative dose of the category. The differences between the slopes were tested using the bootstrap percentile method with 1000 iterations [17]. The data were plotted on a semi-log axes with the log of relative rate on the y-axis and RT dose on the x-axis. The slope is the change in log relative rate by a unit increase in RT dose, adjusting for the other covariates.

We also sought to better understand the underlying RT characteristics driving the greatest D_m and V_{20} changes with our updated dosimetry. Specifically, for each individual for whom updated dosimetry from H_{Atlas} to H_{Hybrid} resulted in D_m changing (from 30 Gy to 20–29.9 Gy) or V_{20} changing (from >80% to 30–79.9%), we evaluated the following variables: (i) chest RT as yes/no, which includes any field that was directly incident on (a) the chest, and/or (b) head and/or neck and extended inferiorly below the suprasternal notch, and/or (c) abdomen or pelvis and extended superiorly above the diaphragm; and (ii) chest maximum target dose, which was taken as the sum of dose from all overlapping fields, e.g., initial, boost, and recurrence fields treated within 5 years of diagnosis (methods described in Howell et al. [9]). We then stratified the data by primary cancer diagnosis.

All statistical tests were two-sided, with $P < 0.05$ indicating statistical significance. Statistical analyses were done using SAS (version 9.4; SAS Institute, Cary, NC) and R software (version 3.6.0; R Foundation, Vienna, Austria).

Results

Differences in mean heart dose (D_m) computed using H_{Atlas} and H_{Hybrid} are shown with a scatter plot in Fig. 1(a). Overwhelming majority of data points lie below the $D_{Hybrid} = D_{Atlas}$ reference line, indicating that H_{Hybrid} dose estimates are generally lower than H_{Atlas} dose estimates. The histogram of differences in mean heart dose [Fig. 1(b)] supports this fact with majority of changes in the negative direction signifying that the new heart dose estimates by H_{Hybrid} are lower than the previous estimates by H_{Atlas}. Scatter plots and histograms stratified by primary cancer diagnosis are shown in Fig. 2 and Fig. 3, respectively.

With the updated dosimetry, 545 survivors (4.57%) had >10 Gy change in mean heart dose, among whom 19 survivors (0.16%) had >20 Gy change. The majority of these patients were Hodgkin lymphoma survivors (505/545 survivors with >10 Gy change and all 19 survivors with >20 Gy change). Thus, the largest impact of updated dosimetry was observed among Hodgkin lymphoma survivors. Additionally, the 99^{th} and 90^{th} percentiles of decrease in

mean dose for Hodgkin lymphoma survivors was equal to 19.6 Gy and 12.0 Gy, respectively. The second largest impact was observed for central nervous system tumor survivors with the 99th and 90th percentile of decrease in mean dose equal to 9.4 Gy and 7.3 Gy, respectively. The histogram of differences in dose volume metrics (V_5 and V_{20}), stratified by primary cancer diagnosis are plotted in Supplementary Figs. 2 and 3. Consistent with changes in D_m, maximum variations were observed for Hodgkin lymphoma and central nervous system tumor survivors.

Reported in Supplementary Table 1 are mean and standard deviations of the D_m, $V_{20,}$ and V_5 for individuals treated with RT included in our previous (H_{Atlas}, N = 11,960) and current (H_{Hybrid}, N = 11,919) analyses. On average for the CCSS cohort, D_m, V_{20}, and V_5 for H_{Hybrid} compared to H_{Atlas} were 2.1 Gy, 6.5%, and 6.0% lower, respectively.

Cumulative incidence curves (5 to 30 years after primary cancer diagnosis), 30-year cumulative incidence, and adjusted relative rates for developing any cardiac disease, CAD, and HF are reported in Fig. 4, Table 1, and Table 2, respectively. Consistent with our previous findings, when dose–response relationships were reevaluated with H_{Hybrid}, $D_m \geq$ 10 Gy, $V_{20} \geq 0.1\%$ and $V_{5,(V_{20}=0\%)} \geq 50\%$ were associated with increased cumulative incidences and adjusted relative rates for any cardiac disease, CAD, and HF. For most comparisons, the current study reinforced prior results and the updated values were not statistically significantly different between the two heart dosimetry approaches. However, in the 20 to 29.9 Gy dose category for D_m, the 30-year cumulative incidences (Table 1) of any cardiac disease and CAD significantly increased from 7.7 (95%CI: 5.2–10.2) to 13.3 (95%CI: 10.1–16.5) and from 3.7 (95%CI: 1.9–5.4) to 8.4 (95%CI: 5.7–11.1), respectively (both $P < 0.05$). Similarly, in the 20 to 29.9 Gy dose category for D_m, the adjusted relative rates (Table 2) significantly increased from 2.8 (95% CI: 2.0–3.8) to 4.1 (95%CI:3.0–5.5) for any cardiac disease (P = 0.012) and from 3.2 (95%CI: 1.9–5.4) to 5.3 (95%CI: 3.4–8.3) for CAD (P = 0.018); the change for HF was also appreciable, but not statistically significant (P = 0.064), increasing from 2.9 (95% CI:1.9–4.6) to 4.3 (95%CI:2.9–6.5). In the 30% to 79.9% volume category for V_{20}, the 30-year cumulative incidences (Table 1) of any cardiac disease and CAD significantly increased from 8.6 (95%CI: 5.7–11.5) to 12.8 (95%CI: 10.8–14.9) and from 4.7 (95%CI: 2.4–7.1) to 8.8 (95%CI: 6.9–10.6), respectively (both $P < 0.05$). Similarly, in the 30% to 79.9% volume category for V_{20}, the adjusted relative rates (Table 2) increased from 3.3 (95%CI: 2.3–4.8) to 4.3 (95% CI:3.4–5.5) for any cardiac disease (P = 0.034) and from 3.7 (95% CI: 2.1–6.5) to 5.6 (95%CI: 3.8–8.2) for CAD (P = 0.022).

The D_m-specific adjusted RT-dose–response relationships are shown in Fig. 5 (A-C) for any cardiac disease, CAD, and HF for H_{Hybrid} and H_{Atlas}. The data in Fig. 5. are log relative rates from the piecewise exponential models against RT dose, whose slopes plot as straight lines on these semi-log graphs. In all cases, the slopes of the dose response from our current analyses with H_{Hybrid} dosimetry are steeper and significantly different ($P < 0.001$) from slope estimates with H_{Atlas} dosimetry. Dose-response plots analogous to those shown in Fig. 5 were not reported in our previous study. Here we used this graph to visually illustrate differences in dose responses between our previous and current updated dosimetry analyses. We note that the H_{Atlas} data presented in Fig. 5 are unchanged from Bates et al.

Reported in Supplementary Table 2 is a summary of the individuals for whom updated heart dosimetry resulted in significant categorical changes in D_m from ≥ 30 Gy to 20–29.9 Gy and V_{20} from ≥ 80% to 30–79.9%. Our analysis identified that all individuals with categorical changes had chest-directed RT. Among these individuals, average D_m decreased by 10.5 ± 4.3 Gy and 93% (N = 546) had primary cancer diagnoses of Hodgkin lymphoma (86.7%) or central nervous system tumors (6.3%); 97.8 % (N = 574) of these individuals were prescribed chest target doses ≥ 30 Gy. Similarly, on average V_{20} decreased by 27.7 ± 4.2 % and 93.5% (N = 1882) had primary cancer diagnoses of Hodgkin lymphoma (66.6%) or central nervous system cancers (26.9%); >99.9% (N = 2011) were prescribed chest target doses ≥ 20 Gy.

Discussion

In this study, we updated our previous analysis of therapy-related cardiac risk in childhood cancer survivors using RT heart dosimetry data calculated with a more anatomically realistic and validated heart model to provide improved estimates of RT-related late cardiac disease risk. Changes in the dose and dose-volume metrics for each survivor depends on their respective disease, prescribed dose, fields, and blocking etc. Overall, we observed decrease in dose and dose volume metrics with H_{Hybrid} for all survivor groups as shown in Figs. 1–3 and Supplementary Figs. 2–3. The largest changes were observed for Hodgkin lymphoma survivors and central nervous system tumor survivors owing to the higher prescribed dose and types of field/blocking used for these patients.

Broadly, the results of this study are consistent with our previous work in that the risk for late cardiac disease increases with D_m-≥ 10 Gy, V_{20} ≥ 0.1 %, and $V_{5,(V_{20}=0\%)}$ ≥ 50%. For most comparisons, findings were not statistically significantly different between the two approaches. However, there are important differences. In particular, the changes in risk estimates were statistically significant (P < 0.05) for D_m in the category of 20 to 29.9 Gy and for V_{20} in the category of 30% to 79.9%. We also observed steeper slopes of the D_m-specific RT-dose–response relationships of late cardiac disease risk compared to our previous estimates. These findings present a methodological refinement in heart RT dosimetry leading to improved estimates of RT-related late cardiac disease risk. This new insight supports efforts to minimize heart doses for newly diagnosed pediatric cancer patients and better informs cardiac screening guidelines for survivors of childhood cancer.

Our results demonstrate that the statistically significant increases in (H_{Hybrid} versus H_{Atlas} dosimetry) cumulative incidences (Table 1) and adjusted relative rates (Table 2) for D_m in the 20 to 29.9 Gy dose category and the V_{20} in 30 to 79.9% volume category were primarily driven by our previous heart model overestimating D_m and V_{20} (Supplementary Table 2) for individuals with chest-directed RT with prescribed doses > 30 Gy for D_m and ≥20 Gy for V_{20}. Specifically, primarily for Hodgkin lymphoma and central nervous system tumors, for H_{Hybrid}, a larger fraction of heart volume was under the lung blocks or out-of-field (as opposed to H_{Atlas} where almost the entire heart volume was in-field). This is illustrated in Supplementary Fig. 4 for typical T-mantle and mantle fields used for Hodgkin lymphoma and spine fields for central nervous system tumors, resulting in much lower D_m and V_{20} for H_{Hybrid} as opposed to H_{Atlas} (Supplementary Table 2). Conversely, differences in D_m

and V_{20} were much smaller for field types where both heart models were entirely in-field (e.g., whole lung) or entirely out-of-field (e.g., whole brain), and thus had little effect on the dose–response models. Our findings that the dosimetric changes were greatest when the heart was partially in-field are consistent with the studies [18] that reported higher dose reconstruction uncertainty for partially in-field organs.

In our study, we reported that H_{Atlas} systematically overestimated heart D_m compared to H_{Hybrid} with the magnitude of overestimation highest for chest-directed RT. We note that the magnitude of the differences between dosimetry calculated with H_{Atlas} and H_{Hybrid} is larger than the dosimetric uncertainties reported in a recent study by Ntentas et al. (2020) [19]. Ntentas et al. examined the impact of uncertainties in cardiac dose reconstruction for 14 adult Hodgkin lymphoma patients by comparing heart D_m calculated with four different RT reconstruction methods (including ours) to ground truth heart D_m calculated in a commercial treatment planning system using each patient's RT planning CT. There are many differences in study design that make it difficult to directly compare our study with that of Ntentas. First, the heart doses we provided for that study were calculated using H_{Atlas} in 2017, prior to the development of our enhanced heart model. In addition, we applied a patient specific adaptation to the H_{Atlas} model, based on the contemporary RT data available for the Ntentas study. In particular, the contemporary RT records included digitally reconstructed radiographs (DRR) with renderings of the patients' hearts. Thus, we were able to code the position of the superior and inferior aspect of each patient's heart, in addition to coding the specific field parameters for each patient. Each patient's RT fields were then reconstructed on an adult phantom with a patient specific H_{Atlas} model that was shifted superiorly, inferiorly, stretched or shrunk to correspond to the heart contour on their DRR. There were also differences in the cohort composition between our current study and in Ntentas et al. For example, the Ntentas study was for an adult cohort, all of whom were diagnosed with Hodgkin lymphoma and treated with 6 MV mantles, most of which were more contemporary in design, e.g., mini mantles compared to the full mantles used in the CCSS. As previously mentioned, the CCSS cohort considered here included more than 12,000 irradiated individuals aged 21 years or younger and diagnosed with eight different primary pediatric cancers between 1970 and 1999. Also, the CCSS RT included a wide range of photon beam energies, i.e., orthovoltage, Cobalt-60, 4 MV, and 6 MV. These differences in reconstruction methods, organ models, field geometries, beam energies, and age make it difficult to draw direct comparisons between dose reconstruction uncertainties reported from our current study with that reported by Ntentas et al. and other uncertainty analyses in the literature [18]. The challenges associated with such comparisons highlight the complex nature of dose reconstruction uncertainty and that uncertainties cannot be directly translated from one study to another study. Such challenges are particularly complex for pediatric dose reconstructions, due to the greater variation in organ size and shape, which is less prominent in adults. For late effects studies, particularly those including childhood cancer survivors, it is important to use most optimized dose reconstruction methodology possible within the context of available radiotherapy data and resources. A recent review [18] reported that uncertainties can have a large impact on dose–response relationships and recommended quantifying dose reconstruction uncertainties and where possible reducing those uncertainties; our efforts here, align with those recommendations.

We also note that the dosimetric uncertainty observed here was systematic and specific to our heart model's geometry and does not translate to published dosimetry for other organs. Specifically, the systematic underestimation of dose for chest-directed radiation therapy was due to our H_{Atlas} model being laterally smaller compared to the anatomically more realistic H_{Hybrid} model. In future, any new organs that are added to our phantom will be developed following the H_{Hybrid} model development methodology [10], i.e., organ models will be developed using 3D anatomy, e.g., reference phantoms or patients' anatomies.

From a clinical perspective, our findings that cumulative incidences and adjusted relative rates were higher than previously estimated for D_m in the category of 20 to 29.9 Gy and V_{20} in the category of 30% to 79.9% reinforce the importance of contemporary conformal RT to achieve lower heart doses for pediatric patients requiring moderate and high-dose chest-directed RT. Intensity modulated RT, proton therapy and/or field reduction, such as using post-chemotherapy residual volume RT fields are examples of RT techniques that have been shown to reduce heart dose compared to conventional 2D and 3D RT techniques and older large field designs [20,21]. Similarly, for patients receiving craniospinal irradiation, proton therapy essentially eliminates heart dose [22,23]. The findings of our current study support the routine use of cardiac dose mitigation strategies for high-risk Hodgkin lymphoma and craniospinal pediatric patients.

Our data also confirm the findings of our prior studies [2,4] that established the linear relationships between mean cardiac RT dose and risk for late cardiac diseases above 10 Gy. Results from a European study [5] showed mean cardiac RT doses of 5–15 Gy increases the risk of cardiac diseases, but our investigation did not reveal any risk for patients with mean heart doses in the 5–9.9 Gy dose range (data not presented). Our work supports and is in alignment with the international consortium on cardiomyopathy guidelines which reported evidence of increased risk of HF for RT-dose of less than 15 Gy [24].

A limitation of this study (and all studies of long-term survivors) is that heart dose and volume metrics had to be estimated based on treatment field reconstruction on computational phantoms because the individuals in the CCSS were treated in the pre-CT era of RT. However a major strength of this study is that heart doses were estimated for each individual in the study by reconstructing their RT fields on a computational phantom scaled to their age at RT [11] with an anatomically realistic and validated heart model, $H_{Hybrid.}$ We previously reported dosimetric uncertainty in D_m of less than 5% [10], for dose reconstructions with H_{Hybrid} when compared with actual patient (ground truth) CT-based calculations in a commercial treatment planning system. We also previously demonstrated that H_{Hybrid} is representative of pediatric heart anatomy (from infant to adolescent). Another strength of this study is that the CCSS population considered here, is the world's largest multi-institutional cohort for which graded late cardiac disease outcomes are available. Notably, we considered a population of nearly 25,000 survivors of eight different primary pediatric cancers with an extensive range of treatment (chemotherapy and RT) exposures and long-term longitudinal follow-up.

Lastly, we were able to achieve the methodological refinement of heart dosimetry presented here following recent technological advancements within our lab's computational

infrastructure in 2020. Specifically, we adapted our computational phantom, which was developed more than two decades ago from FORTRAN to Digital Imaging and Communications in Medicine (DICOM) format [11]. That adaptation made it possible to register our age-scaled phantom to CT-based gold-standard pediatric phantoms [25,26] and thus to develop the H_{Hybrid} model [10].

In summary, we updated dose–response models for any cardiac disease, CAD, and HF, which are consistent with our previous work in that the risk for late cardiac disease increases with $D_m \geq 10$ Gy, $V_{20} \geq 0.1\%$, and $V_{5,(V_{20}=0\%)} \geq 50\%$, with statistically significant higher risks observed for D_m in the 20 to 29.9 Gy categories and V_{20} in the 30% to 79.9 % volume categories. This finding reinforces the importance of using contemporary conformal RT to achieve lower heart dose and dose volume metrics for pediatric patients requiring high-dose chest-directed RT 20 Gy. Having completed this analysis of the impact of our enhanced cardiac model on previously reported dose response models, we are currently developing cardiac substructure level dose–response models.

Supplementary Material

Refer to Web version on PubMed Central for supplementary material.

Acknowledgments

Funding statement

This work was supported by the National Cancer Institute (CA55727, G.T. Armstrong, Principal Investigator). The MD Anderson Late Effects Group (PI: Dr. Rebecca Howell) receives funding through a subcontract with Childhood Survivor Cancer Study, RFA-CA-15-502, NIH/NCI, PI - Gregory T. Armstrong. Support to St. Jude Children's Research Hospital also was provided by the Cancer Center Support (CORE) grant (CA21765, C. Roberts, Principal Investigator) and the American Lebanese Syrian Associated Charities (ALSAC). Suman Shrestha was awarded the CCSS Career Development Award (2019) and Health Physics Society Robert S. Landauer Sr. Fellowship (2020–2021).

Conflict of interest statement

All authors certify that they have seen and approved the final version of the manuscript being submitted. They also warrant that the article is the authors' original work, has not received prior publication, and is not under consideration for publication elsewhere.

References

[1]. Armstrong GT, Oeffinger KC, Chen Y, Kawashima T, Yasui Y, Leisenring W, et al. Modifiable risk factors and major cardiac events among adult survivors of childhood cancer. J Clin Oncoly 2013;31:3673–80.

[2]. Mulrooney DA, Yeazel MW, Kawashima T, Mertens AC, Mitby P, Stovall M, et al. Cardiac outcomes in a cohort of adult survivors of childhood and adolescent cancer: retrospective analysis of the Childhood Cancer Survivor Study cohort. BMJ 2009;339. b4606.

[3]. Adams MJ, Lipshultz SE. Pathophysiology of anthracycline- and radiation-associated cardiomyopathies: implications for screening and prevention. Pediatr Blood Cancer 2005;44:600–6. [PubMed: 15856486]

[4]. Bates JE, Howell RM, Liu Qi, Yasui Y, Mulrooney DA, Dhakal S, et al. Therapy-related cardiac risk in childhood cancer survivors: an analysis of the childhood cancer survivor study. J Clin Oncol 2019;37:1090–101. [PubMed: 30860946]

[5]. Haddy N, Diallo S, El-Fayech C, Schwartz B, Pein F, Hawkins M, et al. Cardiac diseases following childhood cancer treatment: cohort study. Circulation 2016;133:31–8. [PubMed: 26487757]

[6]. Lipshultz SE, Adams MJ, Colan SD, Constine LS, Herman EH, Hsu DT, et al. Long-term cardiovascular toxicity in children, adolescents, and young adults who receive cancer therapy: pathophysiology, course, monitoring, management, prevention, and research directions: a scientific statement from the American Heart Association. Circulation 2013;128:1927–95. [PubMed: 24081971]

[7]. Mulrooney DA, Armstrong GT, Huang S, Ness KK, Ehrhardt MJ, Joshi VM, et al. Cardiac outcomes in adult survivors of childhood cancer exposed to cardiotoxic therapy: a cross-sectional study. Ann Intern Med 2016;164:93. 10.7326/M15-0424. [PubMed: 26747086]

[8]. Eycleshymer AC, Shoemaker DM. A cross-section anatomy. New York1970.

[9]. Howell RM, Smith SA, Weathers RE, Kry SF, Stovall M. Adaptations to a generalized radiation dose reconstruction methodology for use in epidemiologic studies: an update from the MD Anderson Late Effect Group. Radiat Res 2019;192:169–88. [PubMed: 31211642]

[10]. Shrestha S, Gupta AC, Bates JE, Lee C, Owens CA, Hoppe BS, et al. Development and validation of an age-scalable cardiac model with substructures for dosimetry in late-effects studies of childhood cancer survivors. Radiother Oncol 2020;153:163–71. [PubMed: 33075392]

[11]. Gupta AC, Shrestha S, Owens CA, Smith SA, Qiao Y, Weathers RE, et al. Development of an age-scalable 3D computational phantom in DICOM standard for late effects studies of childhood cancer survivors. Biomed Phys Eng Express 2020;6:065004.

[12]. Stovall M, Weathers R, Kasper C, Smith SA, Travis L, Ron E, et al. Dose reconstruction for therapeutic and diagnostic radiation exposures: use in epidemiological studies. Radiat Res 2006;166:141–57. [PubMed: 16808603]

[13]. Leisenring WM, Mertens AC, Armstrong GT, Stovall MA, Neglia JP, Lanctot JQ, et al. Pediatric cancer survivorship research: experience of the Childhood Cancer Survivor Study. J Clin Oncol 2009;27:2319–27. [PubMed: 19364957]

[14]. Robison LL, Armstrong GT, Boice JD, Chow EJ, Davies SM, Donaldson SS, et al. The Childhood Cancer Survivor Study: a National Cancer Institute-supported resource for outcome and intervention research. J Clin Oncol 2009;27:2308–18. [PubMed: 19364948]

[15]. Robison LL, Mertens AC, Boice JD, Breslow NE, Donaldson SS, Green DM, et al. Study design and cohort characteristics of the Childhood Cancer Survivor Study: a multi-institutional collaborative project. Med Pediatr Oncol 2002;38:229–39. [PubMed: 11920786]

[16]. Gray RJ. A class of K-sample tests for comparing the cumulative incidence of a competing risk. Ann Statistics 1988;16:1141–54.

[17]. Good P. Resampling methods: a practical guide to data analysis. Springer-Verlag. 2006;3rd Edition, New York:5–28.

[18]. Vu~ Bezin J, Allodji RS, Mège JP, Beldjoudi G, Saunier F, Chavaudra, et al. A review of uncertainties in radiotherapy dose reconstruction and their impacts on dose-response relationships. J Radiol Protect. 2017;37:R1–r18.

[19]. Ntentas G, Darby SC, Aznar MC, Hodgson DC, Howell RM, Maraldo MV, et al. Dose-response relationships for radiation-related heart disease: Impact of uncertainties in cardiac dose reconstruction. Radiother Oncol 2020;153:155–62. [PubMed: 32890611]

[20]. Hoppe BS, Mailhot Vega RB, Mendenhall NP, Sandler ES, Slayton WB, Katzenstein H, et al. Irradiating residual disease to 30 Gy with proton therapy in pediatric mediastinal Hodgkin Lymphoma. Int J Particle Ther. 2020;6:11–6.

[21]. Hoppe BS, Bates JE, Mendenhall NP, Morris CG, Louis D, Ho MW, et al. The meaningless meaning of mean heart dose in mediastinal lymphoma in the modern radiation therapy era. Pract Radiat Oncol 2020;10:e147–54. [PubMed: 31586483]

[22]. Howell RM, Giebeler A, Koontz-Raisig W, Mahajan A, Etzel CJ, D'Amelio AM, et al. Comparison of therapeutic dosimetric data from passively scattered proton and photon craniospinal irradiations for medulloblastoma. Radiat Oncol (London, England) 2012;7:116.

[23]. Zhang R, Howell RM, Taddei PJ, Giebeler A, Mahajan A, Newhauser WD. A comparative study on the risks of radiogenic second cancers and cardiac mortality in a set of pediatric

medulloblastoma patients treated with photon or proton craniospinal irradiation. Radiother Oncol 2014;113:84–8. [PubMed: 25128084]

[24]. Armenian SH, Hudson MM, Mulder RL, Chen MH, Constine LS, Dwyer M, et al. Recommendations for cardiomyopathy surveillance for survivors of childhood cancer: a report from the International Late Effects of Childhood Cancer Guideline Harmonization Group. Lancet Oncol 2015;16:e123–36. [PubMed: 25752563]

[25]. Geyer AM, O'Reilly S, Lee C, Long DJ, Bolch WE. The UF/NCI family of hybrid computational phantoms representing the current US population of male and female children, adolescents, and adults—application to CT dosimetry. Phys Med Biol 2014;59:5225–42. [PubMed: 25144322]

[26]. Lee C, Lodwick D, Hurtado J, Pafundi D, Williams JL, Bolch WE. The UF family of reference hybrid phantoms for computational radiation dosimetry. Phys Med Biol 2010;55:339–63. [PubMed: 20019401]

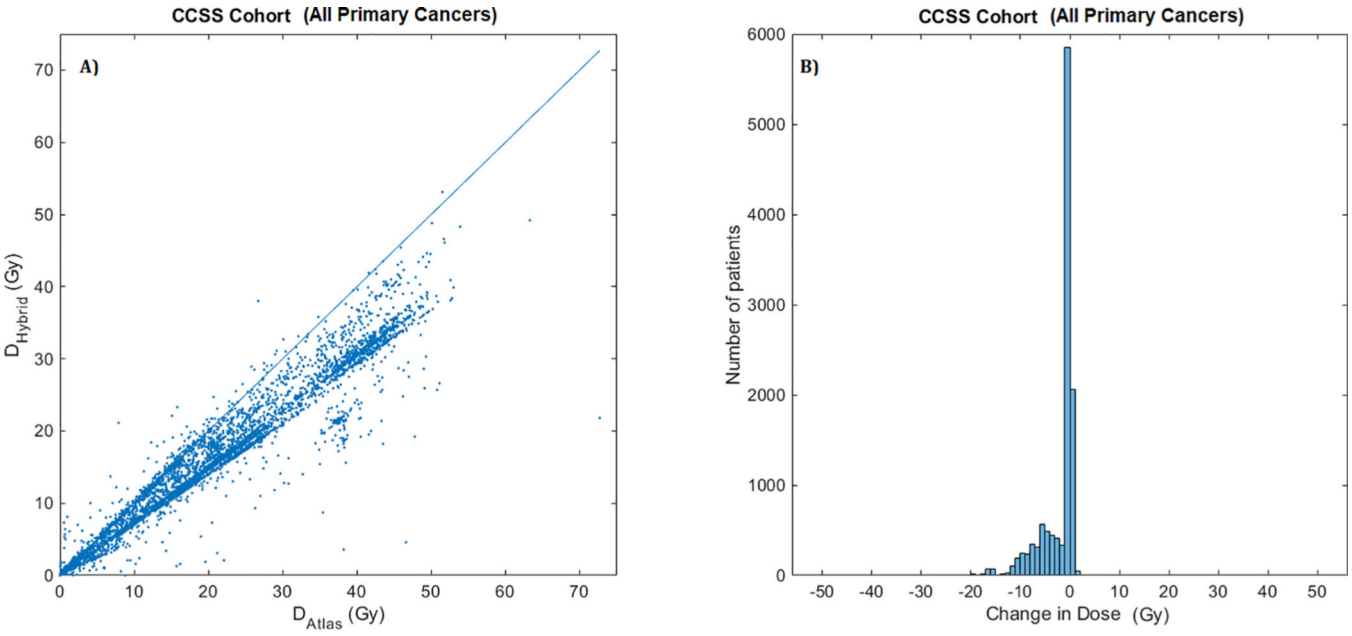

Fig. 1.

(a). Scatter plot of mean heart dose (in Gy:Gray) estimated using H_{Hybrid} (on *y*-axis) *vs.* H_{Atlas} (on *x*-axis) for the entire CCSS cohort (all primary cancers). The line marks the equality of the two estimated doses, $D_{Hybrid} = D_{Atlas}$. Points below the lines indicate lower dose estimate with H_{Hybrid} dosimetry. (b) Histogram of differences in mean heart dose, $D_{Hybrid} - D_{Atlas}$. Cluster of patients with negative values indicate lower dose estimates with H_{Hybrid}.

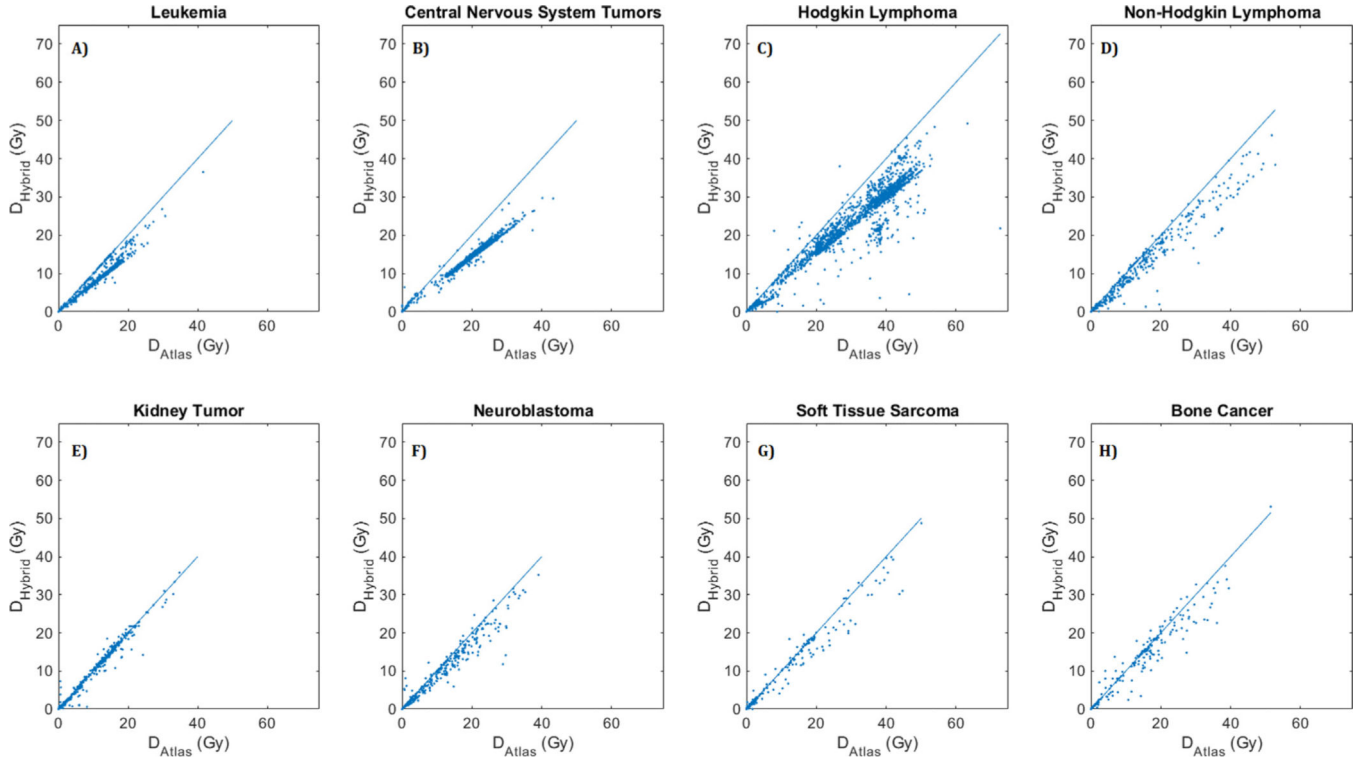

Fig. 2.

Scatter plot of mean heart dose (in Gy:Gray) calculated using H_{Hybrid} (on *y*-axis) *vs.* H_{Atlas} (on *x*-axis) for survivors of (A) Leukemia, (B) Central Nervous System Tumors, (C) Hodgkin Lymphoma, (D) Non-Hodgkin Lymphoma, (E) Kidney Tumor, (F) Neuroblastoma, (G) Soft Tissue Sarcoma, and (H) Bone Cancer. The line marks the equality of the two estimated doses, $D_{Hybrid} = D_{Atlas}$. Points below the lines indicate lower dose estimates with H_{Hybrid} dosimetry.

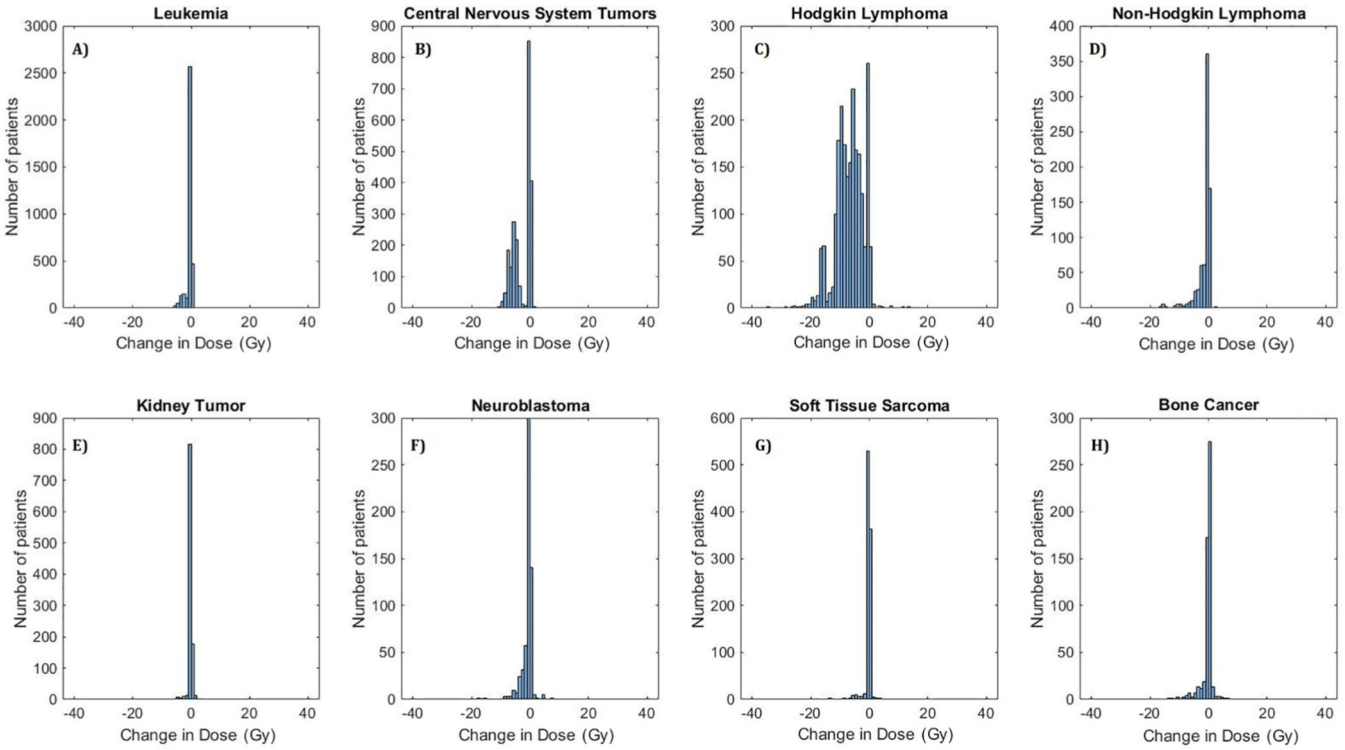

Fig. 3.

Histogram of differences in mean heart dose (in Gy:Gray), $H_{Hybrid} - H_{Atlas}$, for survivors of (A) Leukemia, (B) Central Nervous System Tumors, (C) Hodgkin Lymphoma, (D) Non-Hodgkin Lymphoma, (E) Kidney Tumor, (F) Neuroblastoma, (G) Soft Tissue Sarcoma, and (H) Bone Cancer. Cluster of patients with negative values indicate lower dose estimates with H_{Hybrid}.

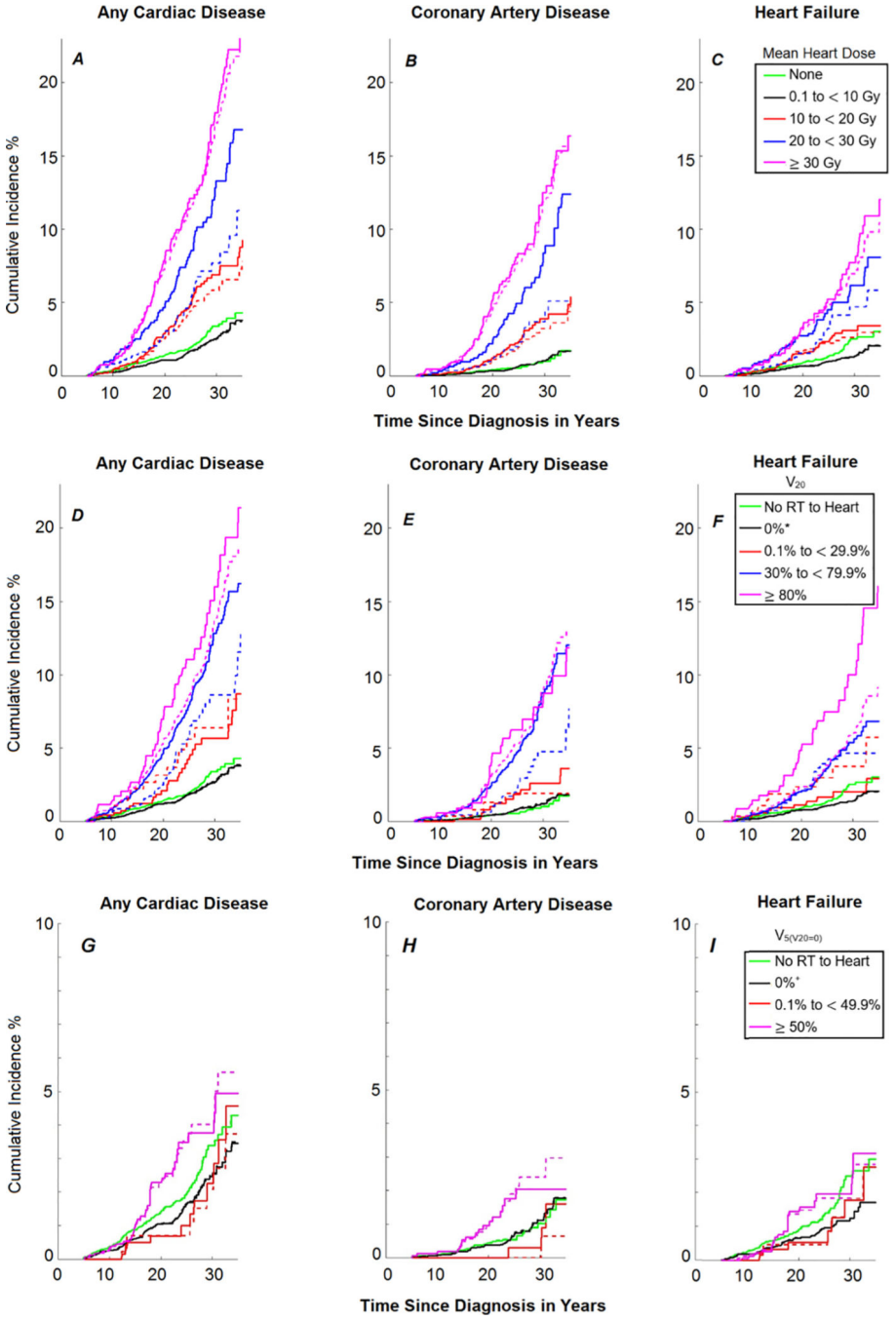

Fig. 4.

Cumulative incidence curves (5–30 years since primary cancer diagnosis) of developing any cardiac disease, coronary artery disease, and heart failure based on (A–C) mean heart dose (Gy), (D–F) percentage of heart volume (%) receiving ≥ 20 Gy (V_{20}), and (G–I) percentage of heart volume (%) ≥ 5 Gy but < 20 Gy ($V_{5,(V20=0\%)}$). Note scales of the vertical axis are different for panels G, H, and I. Dashed lines correspond to Bates et al. 2019 [4] using H_{Atlas} and solid lines correspond to this work using H_{Hybrid}. *indicates maximum RT dose to heart of 0.1 to 19.9 Gy; $^{+}$indicates maximum RT dose to heart of 0.1 to 4.9 Gy.

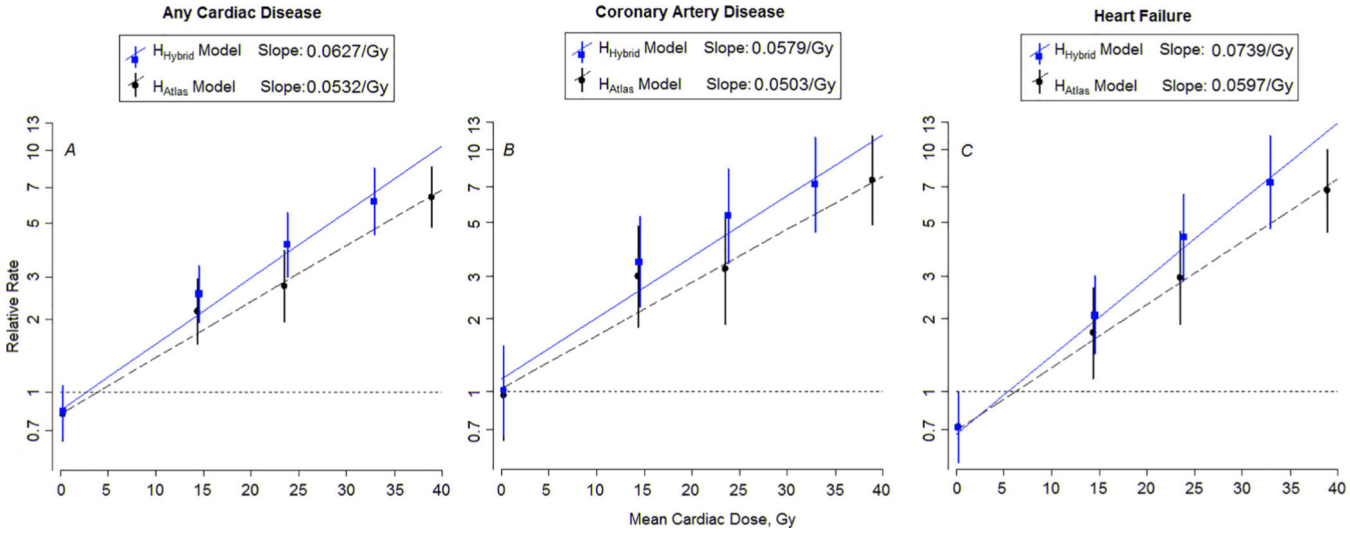

Fig. 5.

The D_m-specific adjusted relative rates and RT-dose–response relationships (lines) for any cardiac diseases, coronary artery disease and heart failure based on (A–C) mean heart dose (Gy). Symbols (squares and circles) represent rate ratios from categorical model (error bars represent 95% confidence interval) for the dose categories of (0.1– 9.9), (10–19.9), (20–29.9), (≥30) Gy, represented at the median doses of 0.26, 14.4, 23.5, and 38.9 Gy for the H_{Atlas} dosimetry and at 0.22, 14.5, 23.8, 32.9 Gy for the updated H_{Hybrid} dosimetry. The horizontal dashed line corresponds to a relative rate of 1.0. The H_{Hybrid} data are plotted with blue font, with solid line and square symbols. H_{Atlas} data are plotted in black font with dashed lines and circle symbols. The slopes were significantly different ($P < 0.001$) for H_{Hybrid} and H_{Atlas} in each case. Here we have used the standard log-rate model for time-to-event data (i.e., piecewise exponential model), where the log event rate is modeled as linear in covariate effects. In our case, event refers to cardiovascular late effect events. Mathematically, $\log(\text{rate}) = b_0 + b_1 * I(\text{dose} > 0 \text{ indicator}) + b_2 * \text{dose} + \text{all the other covariates}$.

Radiother Oncol. Author manuscript; available in PMC 2022 April 25.

Table 1

Comparison of cumulative incidence (%) at 30 years since primary cancer diagnosis for Grade 3 to 5 of any cardiac disease among 5-year survivors of childhood cancer by mean heart doses (D_m), percentage of heart volume (%) receiving ≥ 20 Gy (V_{20}), and percentage of heart volume (%) ≥ 5 Gy but < 20 Gy ($V_{5,(V_{20}=0\%)}$), using H_{Atlas} versus H_{Hybrid}.

Variable	Any Cardiac Disease			Coronary Artery Disease			Heart Failure		
	Cumulative Incidence (95% CI)		*P*	Cumulative Incidence (95% CI)		*P*	Cumulative Incidence (95% CI)		*P*
D_m (Gy)	**H_{Atlas} (Bates *et al.*)**	**H_{Hybrid} (This Work)**		**H_{Atlas} (Bates *et al.*)**	**H_{Hybrid} (This Work)**		**H_{Atlas} (Bates *et al.*)**	**H_{Hybrid} (This Work)**	
No RT*	3.4 [2.6 – 4.1)	3.4 [2.6 – 4.2)	0.238	1.0 [0.6 – 1.5)	1.0 [0.6 – 1.5)	0.244	2.5 [1.8 – 3.2)	2.5 [1.8 – 3.2)	0.242
0.1 – 9.9	2.6 [2.0 – 3.1)	2.6 [2.1 – 3.1)	0.410	1.0 [0.7 – 1.4)	1.0 [0.7 – 1.4)	0.500	1.4 [1.0 – 1.7)	1.4 [1.0 – 1.7)	0.820
10 – 19.9	5.8 [4.2 – 7.4)	6.9 [5.3 – 8.4)	0.074	3.2 [1.9 – 4.5)	3.9 [2.6 – 5.2)	0.126	2.6 [1.6 – 3.6)	3.1 [2.1 – 4.1)	0.232
20 – 29.9	7.7 [5.2 – 10.2)	13.3 [10.1 – 16.5)	0.002	3.7 [1.9 – 5.4)	8.4 (5.7 – 11.1)	0.002	4.7 [2.7 – 6.7)	6.2 [4.0 – 8.3)	0.192
≥30	17.3 (14.5 – 20.0)	18.0 [14.2 – 21.7)	0.600	11.9 [9.5 – 14.2)	12.5 [9.2 – 15.8)	0.590	6.9 [5.2 – 8.7)	7.7 (5.1 – 10.3)	0.348
V_{20} (%)									
No RT*	3.4 [2.6 – 4.1)	3.4 [2.6 – 4.2)	0.238	1.0 [0.6 – 1.5)	1.0 [0.6 – 1.5)	0.244	2.5 [1.8 – 3.2)	2.5 [1.8 – 3.2)	0.242
0%≠	2.8 [2.3 – 3.3)	2.7 [2.2 – 3.2)	0.234	1.2 [0.9 – 1.6)	1.2 [0.8 – 1.5)	0.156	1.4 [1.1 – 1.8)	1.4 [1.1 – 1.8)	0.272
0.1% – 29.9%	6.4 [2.9 – 9.9)	5.7 (3.3 – 8.0)	0.566	1.9 [0.0 – 3.8)	2.6 [0.9 – 4.2)	0.490	3.7 [1.1 – 6.4)	2.0 [0.7 – 3.3)	0.030
30% – 79.9%	8.6 [5.7 – 11.5)	12.8 [10.8 – 14.9)	0.002	4.7 [2.4 – 7.1)	8.8 (6.9 – 10.6)	<0.001	4.6 [2.7 – 6.6)	5.4 [4.1 – 6.7)	0.410
;≥80%	13.7 [11.5 – 15.8)	16.0 [10.6 – 21.4)	0.322	8.9 [7.1 – 10.7)	7.8 (4.1 – 11.5)	0.500	5.8 [4.4 – 7.2)	10.0 [5.7 – 14.3)	0.034
$V_{5,(V_{20}=0\%)}$									
No RT*	3.4 [2.6 – 4.1)	3.4 [2.6 – 4.2)	0.238	1.0 [0.6 – 1.5)	1.0 [0.6 – 1.5)	0.244	2.5 [1.8 – 3.2)	2.5 [1.8 – 3.2)	0.242
0%†	2.6 [2.0 – 3.1)	2.5 [2.0 – 3.1)	0.464	1.1 [0.7 – 1.5)	1.1 [0.7 – 1.5)	0.714	1.3 [0.9 – 1.6)	1.3 [0.9 – 1.6)	0.840
0.1% – 49.9%	2.1 [0.3 – 3.8)	2.3 [0.6 – 3.9)	0.632	0.0 [0.0 – 0.0)	0.3 [0.0 – 0.9)	0.714	1.8 [0.2 – 3.5)	1.8 [0.2 – 3.3)	0.798
≥50%	4.0 [2.6 – 5.4)	3.8 [2.4 – 5.1)	0.506	2.4 [1.2 – 3.5)	2.0 [1.0 – 3.1)	0.274	1.8 [1.0 – 2.7)	2.0 [1.1 – 2.9)	0.104

*No radiation therapy (RT);

†maximum RT dose to heart of 0.1 to 4.9 Gy;

[≠]Indicates maximum RT dose to heart of 0.1 to 19.9 Gy.

Abbreviations: Gray (Gy), 95% Confidence Interval (95% CI).

The P values reported in this table are from the bootstrap inference and indicate statistical significance of the differences in 30-year cumulative incidences obtained using H_{Atlas} versus H_{Hybrid}; $P < 0.05$ and $0.05 \leq P < 0.10$ are shown in green and blue fonts, respectively.

Table 2

Comparison of adjusted relative rates for Grade 3 to 5 cardiac disease among 5-year survivors of childhood cancer by mean heart doses (D_m), percentage of heart volume (%) receiving ≥ 20 Gy (V_{20}), and percentage of heart volume (%) ≥ 5 Gy but < 20 Gy ($V_{5,(V_{20}=0\%)}$)using H_{Atlas} versus H_{Hybrid}.

	Any Cardiac Disease			Coronary Artery Disease			Heart Failure		
	Relative Rates (95% CI)		*P*	Relative Rates (95% CI)		*P*	Relative Rates (95% CI)		*P*
Variable D_m (Gy)	**H_{Atlas} (Bates *et al.*)**	**H_{Hybrid} (This Work)**		**H_{Atlas} (Bates *et al.*)**	**H_{Hybrid} (This Work)**		**H_{Atlas} (Bates *et al.*)**	**H_{Hybrid} (This Work)**	
No RT*	Ref	Ref	N/A	Ref	Ref	N/A	Ref	Ref	N/A
0.1 – 9.9	0.8 (0.6 – 1.1)	0.8 (0.6 – 1.1)	0.348	1.0 (0.6 – 1.5)	1.0 (0.7 – 1.5)	0.254	0.7 (0.5 – 1.0)	0.7 (0.5 – 1.0)	0.548
10 – 19.9	2.2 (1.6 – 2.9)§	2.6 (2.0 – 3.3)§	0.066	3.0 (1.9 – 4.8)§	3.4 (2.2 – 5.3)§	0.286	1.7 (1.1 – 2.7)§	2.1 (1.4 – 3.0)§	0.148
20 – 29.9	2.8 (2.0 – 3.8)§	4.1 (3.0 – 5.5)§	0.012	3.2 (1.9 – 5.4)§	5.3 (3.4 – 8.3)§	0.018	2.9 (1.9 – 4.6)§	4.3 (2.9 – 6.5)§	0.064
≥30	6.4 (4.8 – 8.5)§	6.1 (4.5 – 8.4)§	0.618	7.5 (4.9 – 11.4)§	7.1 (4.6 – 11.2)§	0.628	6.7 (4.6 – 9.9)§	7.3 (4.7 – 11.4)§	0.580
V_{20} (%)									
NoRT*	Ref	Ref	N/A	Ref	Ref	N/A	Ref	Ref	N/A
0%#	0.9 (0.7 – 1.1)	0.9 (0.7 – 1.1)	0.140	1.2 (0.8 – 1.8)	1.1 (0.8 – 1.7)	0.128	0.8 (0.6 – 1.0)	0.7 (0.5 – 1.0)	0.654
0.1% – 29.9%	2.4 (1.4 – 4.2)§	2.4 (1.6 – 3.6)§	0.946	2.1 (0.7 – 5.9)	2.7 (1.4 – 5.0)§	0.574	2.3 (1.1 – 4.8)§	1.7 (0.9 – 3.2)	0.170
30% – 79.9%	3.3 (2.3 – 4.8)§	4.3 (3.4 – 5.5)§	0.034	3.7 (2.1 – 6.5)§	5.6 (3.8 – 8.2)§	0.022	3.4 (2.1 – 5.6)§	4.0 (2.9 – 5.6)8	0.382
£80%	4.5 (3.5 – 5.7)§	4.2 (2.8 – 6.2)§	0.698	5.6 (3.8 – 8.2)§	4.6 (2.5 – 8.2)§	0.364	4.5 (3.2 – 6.2)§	5.6 (3.5 – 8.9)8	0.218
$V_{5,(V_{20}=0\%)}$									
No RT*	Ref	Ref	N/A	Ref	Ref	N/A	Ref	Ref	N/A
0%+	0.8 (0.6 – 1.0)	0.8 (0.6 – 1.1)	0.200	1.0 (0.7 – 1.6)	1.1 (0.7 – 1.7)	0.030	0.6 (0.5 – 0.9)	0.7 (0.5 – 0.9)	0.604
0.1% – 49.9%	0.7 (0.3 – 1.5)	0.7 (0.4 – 1.5)	0.818	0.3 (0.0 – 2.4)	0.5 (0.1 – 2.2)	0.540	0.7 (0.3 – 1.8)	0.7 (0.3 – 1.7)	0.924
≥50%	1.6 (1.1 – 2.3)§	1.5 (1.0 – 2.2)≠	0.220	2.3 (1.3 – 4.0)§	2.0 (1.1 – 3.7)§	0.276	1.3 (0.8 – 2.2)	1.3 (0.8 – 2.2)	0.824

*No radiation therapy (RT);

+indicates maximum RT dose to heart of 0.1 to 4.9 Gy;

[#] indicates maximum RT dose to heart of 0.1 to 19.9 Gy.

Abbreviations: Gray (Gy), 95% Confidence Interval (95% CI).

Significantly elevated adjusted relative rates are indicated with the symbol

[§] for $P < 0.05$ and the symbol

[‡] for $0.05 \leq P < 0.10$.

The P values reported in this table indicate statistical significance of the differences in the adjusted relative rates obtained using H_{Atlas} versus H_{Hybrid}; $P < 0.05$ and $0.05 \leq P < 0.10$ are shown in green and blue fonts, respectively.